

vacuum interactions is given by E. A. Power, *Introductory Quantum Electrodynamics* (American Elsevier, New York, 1964).

⁴Standard microwave notation is used. Cf. J. D. Jackson, *Classical Electrodynamics* (Wiley, New York, 1975), 2nd ed.

⁵S. Haroche, in *Atomic Physics 7*, edited by D. Kleppner and F. M. Pipkin (Plenum, New York, 1981) p.

181.

⁶D. Kleppner, in Proceedings of the Les Houches Summer School, edited by J. C. Adams and R. Ballian (Gordon and Breach, New York, to be published).

⁷H. B. G. Casimir and D. Poulter, *Phys. Rev.* **73**, 360 (1948); see also Ref. 3.

⁸*Radiative Theory and Quantum Electrodynamics*, edited by A. O. Barut (Plenum, New York, 1980).

Polarized Sodium Nuclei Produced by Laser Optical Pumping with Velocity Changing Collisions

P. G. Pappas, R. A. Forber, W. W. Quivers, Jr., R. R. Dasari, and M. S. Feld
*Spectroscopy Laboratory and Physics Department, Massachusetts Institute of Technology,
Cambridge, Massachusetts 02139*

and

D. E. Murnick^(a)

Bell Laboratories, Murray Hill, New Jersey 07974

(Received 3 April 1981)

Theoretical and experimental studies of nuclear polarization induced by single-mode-laser optical pumping are reported. The nuclear polarization is shown to depend on the product of laser intensity and buffer-gas pressure. In ²³Na it approaches one at modest laser intensities (~ 100 mW/cm²) for pressures as small as a few hundred millitorr.

PACS numbers: 32.80.Bx, 29.25.Cy, 29.25.Kf

It has recently been emphasized that achieving complete nuclear polarization in dense alkali vapors is important for producing intense polarized light-ion beams by charge exchange¹ and polarized targets for parity-nonconservation studies.² The present paper demonstrates that single-mode-laser optical pumping in combination with velocity-changing collisions (vcc) can be used to attain a high degree of nuclear polarization in alkali vapors. General theoretical results are presented for alkalilike systems and confirmed in sodium, where almost complete nuclear polarization is achieved. Several authors have studied vcc processes in laser saturation spectroscopy^{3,4} and in laser optical pumping.^{5,6} Complete optical pumping has been achieved at high buffer-gas pressures (collision-broadened regime, where vcc processes have no influence),^{7,8} but the use of laser optical pumping with vcc, at very low buffer pressures, to produce nuclear polarization has not been studied in detail previously.

The laser optical-pumping process, in which nuclear polarization is achieved through the coupling between electron and nuclear spins, has been referred to as laser-induced nuclear orienta-

tion (LINO).⁹ Ordinarily, single-mode laser radiation interacts only with a small fraction of the thermal velocity distribution, of order $\gamma/ku \sim 10^{-2}$, with γ and ku the homogeneous and Doppler widths, respectively. This results in poor Doppler coverage, hence incomplete nuclear polarization. Furthermore, in alkali atoms the atomic population is distributed in two ground-state hyperfine (hf) levels, the Doppler-broadened absorption profiles of which overlap in the cases of Li and Na.

The present experiments use vcc induced by argon buffer-gas atoms to attain single-mode laser optical pumping of the entire ground-state population. In the vcc regime velocity changes cause every alkali atom to be at the resonant velocity at some time during its diffusion through the laser beam. Furthermore, this spatial diffusion considerably retards wall relaxation and greatly extends the laser-atom interaction time. Because of large collision cross sections high vcc rates can be achieved at low (< 1 Torr) buffer pressures, where collisional broadening is negligible.

Consider a gas of three-level atoms with closely spaced or degenerate levels 1 and 2 optically con-

nected to level 0 undergoing vcc [Fig. 1(a)], subjected to resonant single-mode dye-laser radiation of intensity I . For alkali atoms levels 1 and 2 can be either hf levels ($F = 1, 2$ for ^{23}Na) or degenerate M_F states. The laser optical pumping process can be modeled by a set of coupled rate equations¹⁰ for $n_j(v)$, the population density of level j at velocity v , containing the usual terms describing laser pumping: stimulated emission/absorption, radiative decay, and relaxation, the latter due, in this case, to diffusion to the cell walls. In addition, one must include terms describing vcc processes, in which atoms are exchanged among different velocity groups. This model is easily analyzed in the limit of strong collisions, in which the velocity distribution of an atom immediately after a collision is thermal, independent of the atom's initial velocity. In this case the net vcc rate into a given velocity group, $\partial n_j(v)/\partial t|_{\text{vcc}} = \Gamma_v [G(v)N_j - n_j(v)]$, with vcc rate Γ_v , $N_j = \int n_j(v)dv$ the total population density of level j , and $G(v)$ the normalized thermal velocity distribution function. A straightforward calculation of the steady-state population distribution of level 2, in the limit where the spontaneous emission rate $1/\tau$ and $\Gamma_v \gg$ diffusion rate $1/T$, the limit of interest in the experiments, gives

$$n_2(v) = \frac{N_2^0 G(v)}{1 + I/I_{0p}} \left\{ 1 - \left[\frac{L(v)}{1 + I/I_s} \right] \right\}, \quad (1a)$$

where N_2^0 is the total population density of level 2 for $I = 0$, and the characteristic saturation intensities are $I_{0p} = (\rho \hbar \omega / \sigma_D T)(1 + I/I_s)^{1/2}$ and $I_s = \rho \hbar \omega \Gamma_v / \sigma_H$ (in the limit $\tau^{-1} > \Gamma_v$), with σ_D (σ_H) the Doppler (homogeneous) absorption cross section and $\rho = 1/\Gamma_1 \tau$. The dimensionless Lorentzian line-shape factor is

$$L(v) = \frac{(\gamma/2)^2 (1 + I/I_s)}{(\Delta - kv)^2 + (\gamma/2)^2 (1 + I/I_s)}, \quad (1b)$$

with Δ the laser detuning from the atomic center

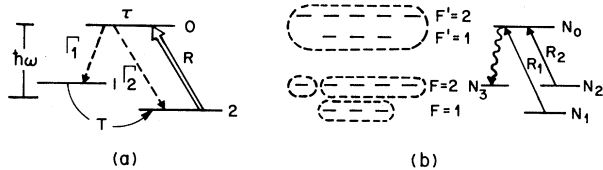


FIG. 1. (a) Optical pumping of three-level system. R is the pumping rate, Γ_1 and Γ_2 are the radiative decay rates ($\Gamma_1 + \Gamma_2 = 1/\tau$), and T is the 2-1 relaxation time. (b) M_F states involved in the ^{23}Na D_1 transition and their grouping into four levels.

frequency.¹¹

The first term of Eq. (1a) describes the depletion of level 2 over the entire velocity distribution due to optical pumping with vcc processes. The second term describes the narrow residual depletion "burned" into the velocity profile at $kv = \Delta$, the saturated width of which is given by $k\delta v = \gamma(1 + I/I_s)^{1/2}$. For $I > I_{0p}$ most of the population in level 2 is depleted over the entire velocity distribution and transferred to level 1. When $I_s \gg I_{0p}$, as in our experiments, the second term (residual depletion) is always negligible. Thus there is no explicit dependence of the level populations on the vcc rate and optical pumping occurs uniformly across the entire Doppler profile [$n_2(v) = N_2 G(v)$].

The above situation gives rise to the most efficient optical pumping, and is thus ideal for producing highly polarized vapors. It also makes possible an important simplification, since with $n_j(v) = N_j G(v)$ the rate equations can be integrated over velocity directly to obtain differential equations for the N_j . The resulting equations are the same in form as the n_j equations, except that the vcc terms are absent and the stimulated emission/absorption rate per atom becomes $\sigma_D I / \hbar \omega$ (instead of $\sigma_H I / \hbar \omega$, as it is in the absence of diffusion). Thus in this limit the rate equations are the same as for a broadband source.

Consider now the optical pumping of the ^{23}Na D_1 transition ($\lambda = 5896 \text{ \AA}$) by right circularly polarized monochromatic light in the limit where complete Doppler coverage is achieved via vcc. This situation is more complex than the three-level case discussed above because of the ^{23}Na 1772-MHz ground-state hf splitting, which gives rise to two pairs of hf components whose Doppler widths (~ 1500 MHz full width at half maximum) overlap. To insure that both ground-state hf levels are pumped the laser frequency is tuned midway between the overlapping $F = 2$ and $F = 1$ hyperfine Doppler profiles ($\Delta_0 = 1772/2$ MHz). To simplify the calculation the sixteen M_F states involved are modeled by the four-level system of Fig. 1(b), with N_j the total population of level j . N_0 consists of the eight M_F states belonging to the $F' = 2$ and $F' = 1$ upper levels, N_1 contains the three M_F states of the $F = 1$ ground-state level, N_2 contains the four $F = 2$ ground states $M_F = -2, -1, 0,$ and 1 which are pumped by the circularly polarized radiation, and N_3 is the population of the $F = 2, M_F = +2$ state, to which the atoms are pumped. In the model the rate equations for the sixteen M_F states are grouped into four N_j rate

equations, with the assumption that the different M_F states within a group have equal populations. Although this approximation does not strictly hold at the low buffer pressures used, its influence on the value predicted for the M_F state being pumped (level 3) is negligible.¹² The steady-state solution of these four coupled equations, neglecting terms of order τ/T , yields

$$\frac{N_3}{N_{\text{total}}} = \frac{0.14(I/I_{op}')^2 + 0.75(I/I_{op}') + 1}{0.14(I/I_{op}')^2 + 3.33(I/I_{op}') + 8}, \quad (2)$$

where $I_{op}' = \hbar\omega/\sigma_D T$, with $\sigma_D = (3\lambda^2/4\pi)(\pi/ku\tau)^{1/2} \times \exp - (\Delta_0/ku)^2$. Note that the nuclei of atoms pumped into level 3 are completely polarized, since in the $M_F = +2$ state $M_I = +\frac{3}{2}$. Thus, the extent of nuclear polarization is completely determined by I/I_{op}' .

For a cylinder of length L and radius a the diffusion time is given by $T_a = p/[(\pi/L)^2 + (2.4/a)^2]D$,¹³ with D the diffusion constant for sodium diffusing through argon buffer.¹⁴ In our experiment the laser beam, radius r , only illuminates the central region of the cell, radius R . An approximate calculation shows that T (needed to compute I_{op}') is then given by $T = T_r + tr^2/(R^2 - r^2)$, with t the diffusion time to the walls in the nonilluminated region. Since $r^2 \ll R^2$, t can be approximated by T_R without compromising the accuracy of the data. Note that T increases linearly with buffer-gas pressure, as both T_r and T_R are proportional to p . Hence N_3 is a function of $I \cdot p$ only. For our experimental parameters Eq. (2) becomes

$$\frac{N_3}{N_{\text{total}}} = \frac{1.92(I \cdot p)^2 + 2.80(I \cdot p) + 1}{1.92(I \cdot p)^2 + 12.48(I \cdot p) + 8} \quad (3)$$

with I in mW/cm^2 and p in Torr. This expression is valid at buffer pressures sufficiently small so that the absorption lines remain Doppler broadened ($\Delta\nu_{\text{Na-Ar}} \approx 30 \text{ MHz/Torr}$), yet large enough so that the atoms move via diffusion (producing a broad probe signal in which the narrow residual depletion is small).

The experiments used circularly polarized radiation from a single-mode cw dye laser to pump the D_1 hf transitions of an optically thin sample (peak small signal absorption 30%) of sodium vapor which also contained up to several Torr of argon. The polarization of the sample was measured with use of a copropagating single-mode probe dye laser with the same circular polarization as the pump laser, which scanned the absorption profile of the optically pumped vapor, thereby measuring the relative number of unpolarized

atoms remaining in various velocity groups. The probe beam power was adjusted to 300 nW in a 2.5-mm-diam beam to prevent optical pumping, and the pump beam diameter was telescopically expanded to 7 mm. The cell, a Pyrex cylinder 3 cm in diameter and 3 cm long with optical-quality end windows, was placed in a resistive oven. The entire cell-oven assembly was surrounded by a pair of 14-in.-diam coils to provide a 3-G holding field along the direction of propagation of the laser beam. The pump-laser frequency was fixed at Δ_0 for effective optical pumping, while the frequency of the probe beam was scanned over the D_1 absorption profile. To increase the probe signal-to-noise ratio the pump beam was chopped and phase-sensitive detection was used.

Typical probe absorption traces are shown in Fig. 2. The $I=0$ trace (Fig. 2, curve *a*), for $p=2$ Torr, shows the normal Doppler contour of the D_1 hf components. As the pump intensity increases (Fig. 2, curves *b* and *c*) the vapor becomes more transparent to the probe beam, and for $I > 25 \text{ mW}/\text{cm}^2$ ($I \cdot p > 50 \text{ mW}/\text{cm}^2 \text{ Torr}$) the probe absorption decreases by about 90% over the entire Doppler profile of all hf transitions, indicating the effectiveness of vcc processes. Figure 2, curve *d* shows a trace for $p=0.2$ Torr where, because of incomplete vcc equilibration,

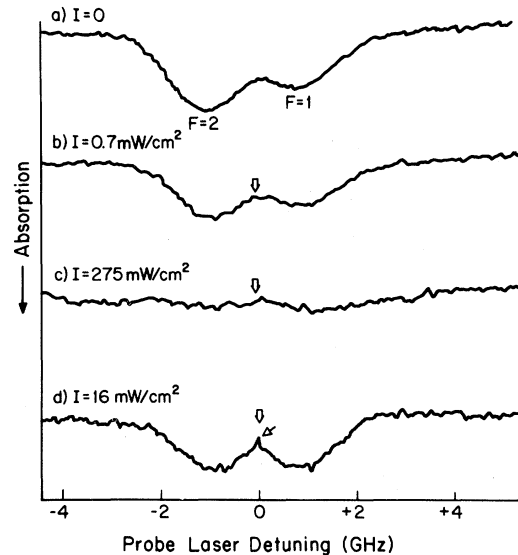


FIG. 2. Curves *a*, *b*, and *c*: Probe absorption at ^{23}Na D_1 transitions for 2.0 Torr of argon at various pump beam intensities. Curve *d*: Same for 0.2 Torr of argon, 16 mW/cm^2 pump intensity. Double arrows mark the frequency of the pump laser; the single arrow indicates the residual Lorentzian depletion.

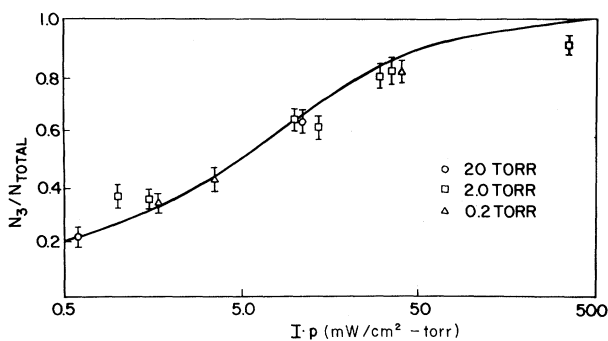


FIG. 3. Relative population of the $F=2$, $M_F=2$ hyperfine level, as a function of $I \cdot p$ in $\text{mW}/\text{cm}^2 \text{ Torr}$.

a small residual depletion remains [Eq. (1)]. This feature becomes progressively larger at lower pressures. Studies to measure vcc cross sections in this intermediate regime are in progress.

Since the present probe measurements do not uniquely establish the population of the individual M_F levels, the simplified four-level model is employed to convert the probe absorption data to experimental values for the population of level 3:

$$N_3/N_{\text{total}} = 1 - \alpha_2/2\alpha_2^0 - 3\alpha_1/8\alpha_1^0, \quad (4)$$

where α_2 and α_1 (α_2^0 and α_1^0) are the peak values of the Doppler-broadened probe absorption coefficients from the $F=2$ and $F=1$ ground-state levels with the pump beam on (off). These values are used to plot N_3/N_{total} vs $I \cdot p$ (Fig. 3). The solid curve shows the theoretical prediction, Eq. (3). As is seen, for $I \cdot p > 50$ about 90% of the ground-state population is transferred to level 3, indicating nearly complete nuclear polarization of the sample.

The small residual unpolarized background which persists, even for large values of $I \cdot p$, may be partly due to stray magnetic fields, to fundamental limits on the optical pumping process, or to both. The oven heating elements, though counterwound, are made of magnetic alloys and produced magnetic-field gradients which are difficult to completely nullify. Transverse magnetic fields mix the M_F levels, thereby reducing the polarization. Elimination of stray magnetic fields and field gradients, and extension of the experiments to optically thick vapors, are currently in progress. In an optically thick vapor alkali-alkali collisions may themselves give rise to a sufficiently large vcc rate for complete optical pumping, obviating the use of foreign buff-

er gas. One must insure, however, that the spin destruction collision rate through alkali-alkali atom collisions is low and, in fact, this process sets an upper limit on vapor density.¹⁵

In conclusion, the present experiments are an important step for polarized-nuclear-target production and clarify the role played by the vcc process in thermalizing the velocity distribution during optical pumping. Polarized alkali targets may be important for the development of the next generation of intense polarized light-ion beams.¹ We are presently developing a polarized ${}^6\text{Li}$ target for parity-nonconservation studies of the reaction ${}^6\text{Li}(\alpha, \gamma){}^{10}\text{B}$.

This work was partially supported by the National Science Foundation and the U. S. Department of Energy. One of us (R.A.F.) is a Howard Hughes Doctoral Fellow.

^(a)Visiting Scientist, Massachusetts Institute of Technology Regional Laser Center, Cambridge, Mass. 02139.

¹G. J. Witteveen, Nucl. Instrum. Methods **158**, 57 (1979).

²D. E. Murnick and M. S. Feld, in *Polarization Phenomena in Nuclear Physics—1980*, edited by G. G. Ohlsen, AIP Conference Proceedings No. 69 (American Institute of Physics, New York, 1981), p. 804.

³P. F. Liao, J. E. Bjorkholm, and P. R. Berman, Phys. Rev. A **21**, 1927 (1980).

⁴R. Vetter, C. Brechignac, and P. R. Berman, Phys. Rev. A **17**, 1609 (1978), and references therein.

⁵M. Pinard, C. G. Aminoff, and F. Laloe, Phys. Rev. A **19**, 2366 (1979).

⁶R. Walkup, A. Spielfiedel, W. D. Phillips, and D. E. Pritchard, Phys. Rev. A **23**, 1869 (1981).

⁷A. C. Tam, J. Appl. Phys. **50**, 1171 (1979).

⁸N. D. Bhaskar, N. Hou, M. Ligare, B. Suleman, and W. Happer, Phys. Rev. A **22**, 2710 (1980).

⁹M. M. Burns, P. G. Pappas, M. S. Feld, and D. E. Murnick, Nucl. Instrum. Methods **141**, 429 (1977).

¹⁰P. G. Pappas, M. M. Burns, D. D. Hinshelwood, M. S. Feld, and D. E. Murnick, Phys. Rev. A **21**, 1955 (1980).

¹¹Equation (1) is obtained from an exact expression (W. W. Quivers, Jr., *et al.*, to be published) in the limit in which terms of order $\Gamma_v \tau$ and $1/\Gamma_v T$ are negligible.

¹²Quivers *et al.*, Ref. 11.

¹³F. B. Hildebrand, *Advanced Calculus for Applications* (Prentice-Hall, New York, 1976), 2nd ed.

¹⁴L. C. Balling, in *Advances in Quantum Electronics*, edited by D. W. Goodwin (Academic, New York, 1975), Vol. 3, p. 1.

¹⁵N. D. Bhaskar, J. Pietras, J. Camparo, W. Happer, and J. Liran, Phys. Rev. Lett. **44**, 930 (1980).